NASA Technical Memorandum 4661

Nonlinear System Guidance in the Presence of Transmission Zero Dynamics

G. Meyer, L. R. Hunt, and R. Su, *Ames Research Center, Moffett Field, California*

JANUARY 1995

National Aeronautics and
Space Administration

Ames Research Center
Moffett Field, CA 94035-1000

CONTENTS

Nomenclature

Acronyms

ATC	air traffic control
CPT	control point table
FVMS	flight vehicle management systems
Greg	guidance regulator
Preg	plant regulator

Symbols

C_{br}	direction cosine matrix of body relative to runway
C_{bt}	direction cosine matrix of body relative to t-axes
C_{tr}	direction cosine matrix of t-axes relative to runway
F_2	generalized force function with trimmed moment
F^f	force function with trimmed moment
f_t^c	t-coordinates of total commanded specific force
f_b^f	body coordinates of total nongravitational specific force, ft/sec^2
f_b^m	body coordinates of total specific moment, rad/sec^2
f_1	generalized translational kinematics
f_2	generalized force function
f_4	generalized moment function
G_0	transfer function of the zero dynamics
g	acceleration of gravity
g_0	Fourier transform inverse of the band limited transfer function G_0
g^α	moment function in terms of Euler angles of C_{bt}
g_1	inverse of f_1 with respect to x_2
g_2	inverse of F_2 with respect to x_3
g_4	moment trim, inverse of f_4 with respect to u_m
h	output function
$h^\pm$	bilateral impulse response
p	configuration parameter
R^m	set of all m-dimensional columns
r_r	runway coordinates of aircraft position
$S(y)$	skew symmetric matrix representing cross product
T	sampling time, sec
$U(t)$	unit step function
u^c	guidance control, corrected for zero dynamics
u^e	feedback control
u^g	guidance control, output of the guidance regulator
u_m	moment control
u^p	plant control
u_p	thrust control
u_f	configuration control
u^0	guidance control for pure feedback model

u_1	commanded generalized translational acceleration $\dot{x}_2$
u_2	commanded generalized angular acceleration $\dot{x}_4$
v_b^a	body coordinates of relative air velocity
v_r	runway coordinates of aircraft velocity
w_r	runway coordinates of wind
x^c	guidance state, corrected for zero dynamics
x^e	guidance state tracking error, $x^g - x^c$
x^g	guidance state, output of the guidance model
x^p	plant state
x^0	guidance state for pure feedback model
y	output
y_c	commanded output
$y^{(k)}$	k^{th} time derivative of y
$y^{[k]}$	y and its first k time derivatives
α_{bt}	Euler angles of C_{bt}
γ	fraction of error corrected at each iteration
δ_i	unit column in direction i
η	solution of the zero dynamics
η^*	approximate time domain solution of the zero dynamics
η^ω	approximate frequency domain solution of the zero dynamics
λ_1	stable eigenvalue
λ_2	unstable eigenvalue
$\phi^{\pm}(t)$	bilateral transition matrix
ψ	acceleration error
ψ_i	acceleration error at i^{th} iteration
ω_{brb}	body coordinates of angular velocity of body relative to runway
ω_s	sampling frequency, rad/sec

Nonlinear System Guidance in the Presence of Transmission Zero Dynamics

G. Meyer, L. R. Hunt, and R. Su

Ames Research Center

Summary

An iterative procedure is proposed for computing the commanded state trajectories and controls that guide a possibly multiaxis, time-varying, nonlinear system with transmission zero dynamics through a given arbitrary sequence of control points. The procedure is initialized by the system inverse with the transmission zero effects nulled out. Then the "steady state" solution of the perturbation model with the transmission zero dynamics intact is computed and used to correct the initial zero-free solution. Both time domain and frequency domain methods are presented for computing the steady state solutions of the possibly nonminimum phase transmission zero dynamics. The procedure is illustrated by means of linear and nonlinear examples.

1 Introduction

This report presents a procedure for guiding a possibly nonlinear system through a schedule of control points. The paradigm is a fully automatic aircraft subject to air traffic control (ATC). The ATC provides a sequence of waypoints through which the aircraft trajectory must pass. The waypoints typically specify time, position, and velocity. The time separation between the waypoints is normally greater than one minute. The flight vehicle management system (FVMS) on board the aircraft is normally aware of at least one waypoint in advance. The FVMS planner provides a sequence of control points between the waypoints so that the aircraft will satisfy additional, vehicle specific constraints. The guidance command generator transforms the schedule of control points into reference state trajectory segments that are flyable and that pass through the control points. These reference trajectories are solutions to the system state equation. The rest of the system is a model follower in which the regulator maintains the aircraft state close to the reference state. Thus, the structure of the complete system is hierarchical: at the top is the ATC; at the bottom are actuators. There is a progressive filling in of the detail as one moves down the hierarchy. In the present report we are concerned with algorithms for transforming the control point schedule into reference state trajectories.

If the system to be controlled is approximately in pure feedback form, that is, if the zero dynamics are negligible, then system inversion provides an effective procedure for the generation of guidance commands (refs. 1 and 2). In their prize paper (ref. 3), Isidori and Byrnes solve the guidance problem in the presence of zero dynamics. However, a solution to a nonlinear partial differential equation must be obtained, and that is not always practical. Furthermore, the commanded output is restricted to outputs of a relaxing autonomous exosystem, whereas we are interested in the case where the output may have discontinuous higher derivatives at the control points. Paden, Chen, and Devasia (refs. 4–6) made a

major advance by finding an iterative solution that avoids the partial differential equation and admits discontinuities at control points.

The solution described in the present paper may be viewed as a modification of the iteration in reference 6. Our procedure consists of two nested iterations. The computation is initialized by the pure feedback solution in which the zero dynamics are nulled out. Then the error resulting from the zero dynamics is removed (outer iteration) by solving a sequence of linear problems. Each linear problem is solved by means of the linear version of the iteration in reference 6. The introduction of the outer iteration allows one to control the effects of nonlinearities on the convergence of the inner iteration. The effectiveness of the approach is illustrated by means of applications to linear, time-varying, and nonlinear systems.

2 System Guidance

The purpose of the guidance subsystem is to generate reference trajectories that will comply with the specifications of a higher-level planner and with the capabilities of the controlled process. Thus, for example, consider a simplified model of the interaction between the ATC and the aircraft under its influence. For simplicity, let both the ATC and all the aircraft be fully automatic. A model of the combined process is shown in figure 1. Based on the available airspace and goals and capabilities of the various aircraft, the ATC provides to each aircraft a sequence of waypoints. The FVMS of each aircraft develops a plan for passing through the assigned waypoints. Then the planner provides a control point table (CPT) of control points that specify the desired conditions at particular times, as well as the aircraft configuration in which the segments are to be flown. The command synthesizer connects the control points by functions of time from a standard set, such as polynomials. The result is the commanded motion of the output y_c and the required time variation of the configuration variables p, such as flaps and landing gear. The guidance generator transforms the desired motion and configuration change (y_c, p) into the complete guidance state trajectory and control (x^g, u^g). The plant regulator transforms the tracking error $\hat{x}^p - x^g$ into a corrective action u^e, which is combined with u^g to produce the plant control u^p. The primary virtue of this model-follower structure is that the regulator is responsible only for controlling the uncertainty arising from disturbance and modeling errors, and not for shaping the plant response. It may be noted that the overall structure is hierarchical with regard to the horizon width and plan refinement and stability. ATC is at the top with the widest horizon, slowest-changing plan, and coarsest specification. The FVMS planner has a narrower horizon and a faster-changing, more refined plan. The guidance generator fills in a lot of detail, and the regulator is at the bottom: it is purely reactive, with the narrowest horizon, and it produces the most refined commands. The ATC plan is stable for minutes, the guidance for seconds, and the regulator for milliseconds, changing at every sample (e.g., 20 msec). In the present report, we are concerned with design of the guidance generator, that is, with the computation of (x^g, u^g).

A high-level description of the guidance problem is straightforward. We are given the system state equation and the output map,

$$\begin{aligned} \dot{x} &= f(x, u, p) \\ y &= h(x, p) \end{aligned} \tag{2-1}$$

where the state $x \in R^n$, the control $u \in R^m$, the parameter $p \in R^k$, and the output $y \in R^m$. We

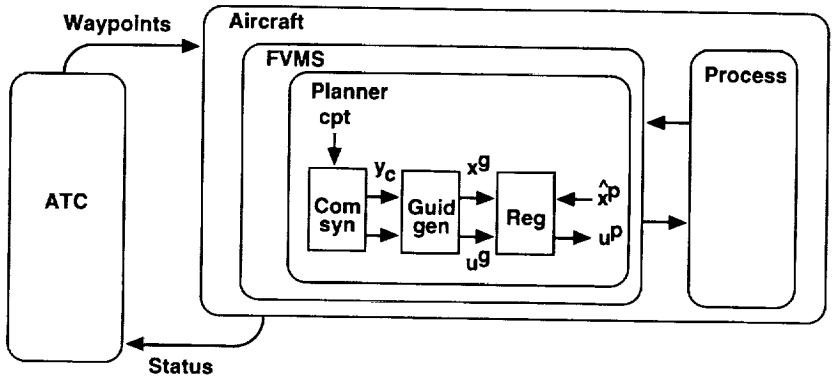

Figure 1. A model of the interaction between ATC and aircraft.

are also given the evolution of the parameter $\{p(t), t \in \mathcal{T}\}$ and the desired evolution of the output $\{y_c(t), t \in \mathcal{T}\}$. The problem is to find a control $\{u^g(t), t \in \mathcal{T}\}$ and the corresponding solution $\{x^g(t), t \in \mathcal{T}\}$ of the state equation so that

$$h[x^g(t), p(t)] = y_c(t) \tag{2-2}$$

Furthermore, the solution (x^g, u^g) should not reach values that are excessive for the task at hand, and the guidance state x^g must be everywhere continuous. It may be noted that since the initial condition x_0^g is not given, the guidance problem is not explicitly an initial value problem.

The following very simple example illustrates the salient features of the guidance problem and the solution approach that will be pursued in the present report.

Example 2–1

Consider a scalar second-order system,

$$\begin{aligned} \dot{x}_1 &= x_2 \\ \dot{x}_2 &= u \\ y &= -x_1 + x_2 \end{aligned} \tag{2-3}$$

that is supposed to track

$$y_c(t) = \sin \omega t \tag{2-4}$$

Obtain a differential equation describing the zero dynamics. Note that there is a nonminimum phase zero at $s = 1$.

$$\begin{aligned} \dot{z} - z &= \sin \omega t \\ x_1 &= z \\ x_2 &= \dot{z} \\ u &= \ddot{z} \end{aligned} \tag{2-5}$$

Consider the initial value problem with the initial condition to be selected later,

$$\begin{aligned} \dot{z} - z &= \sin \omega t \\ z(0) &= z_0 \end{aligned} \tag{2-6}$$

The solution consists of the sum of the homogeneous and particular parts:

$$z = z_h + z_p \tag{2-7}$$

where

$$\begin{aligned} z_h(t) &= ce^t \\ z_p(t) &= a \sin(t + \theta) \end{aligned} \tag{2-8}$$

and where (a, θ) are the gain and phase of the transfer function of the zero dynamics,

$$ae^{j\theta} = (j\omega - 1)^{-1} \tag{2-9}$$

Consequently,

$$z(t) = ce^{t} + a\sin(t + \theta) \tag{2-10}$$

We choose $z(0) = z_p(0)$ in order to obtain $c = 0$ and thus null the homogeneous part. The guidance trajectory is then given by the particular solution,

$$\begin{aligned} x_{1p}(t) &= a\sin(\omega t + \theta) \\ x_{2p}(t) &= a\omega\cos(\omega t + \theta) \\ u_p(t) &= -a\omega^2\sin(\omega t + \theta) \end{aligned} \tag{2-11}$$

The following points should be emphasized:

- In general, the reference y_c as well as the guidance solution may persist indefinitely.
- The reference y_c can be expected to be differentiable at the control points only a small number of times, but the guidance state should be continuous everywhere.
- In the constant linear case, the guidance solution is the particular solution that can be obtained by means of the (possibly unstable) transfer function of the zero dynamics.
- We wish to avoid the computation of the guidance solution by numerical integration of the (possibly unstable) zero dynamics.
- Whereas regulation algorithms must be causal, guidance, being a planning activity, can have noncausal computations.

In the present report we generalize this approach to time-varying and nonlinear systems. The specific case of aircraft guidance is considered, but it should be clear that the methods are applicable to a wider class of systems.

3 Aircraft Model

A rigid body model of an aircraft can be described by the following set of equations:

$$\begin{aligned} \dot{r}_r &= v_r \\ \dot{v}_r &= C_{br}^T f_b^f(u_m, u_p, u_f, v_b^a, \omega_{brb}) + g\delta_3 \\ \dot{C}_{br} &= S(\omega_{brb}) C_{br} \\ \dot{\omega}_{brb} &= f_b^m(u_m, u_p, u_f, v_b^a, \omega_{brb}) \end{aligned} \tag{3-1}$$

where $r_r, v_r \in R^3$ are the runway coordinates of the aircraft center of mass position and velocity, respectively; C_{br} is the direction cosine matrix locating body-fixed axes with respect to the runway; ω_{brb} are the body coordinates of the aircraft angular velocity relative to the runway; $u_m \in R^3$ is the moment control; $u_p \in R^3$ controls the magnitude and direction of engine thrust; and $u_f \in R^3$ represents the aircraft configuration variables such as flaps. Normally not all coordinates of (u_p, u_f) are available for control. The partition into active controls and configuration variables, respectively, is defined by the control mode. Finally, g is the acceleration of gravity, $v_b^a = C_{br}(v_r - w_r)$ are the body coordinates of the air velocity, and w_r are runway coordinates of wind. The force and moment characteristics of the aircraft are described by the force and moment functions (f_b^f, f_b^m). They are typically multiaxis, highly coupled, and nonlinear. It should be noted that the state space is not flat, so coordinate patching may be required for some aircraft maneuvers. A convenient coordinate system is obtained by the introduction of an intermediate axis system, such as the nominal stability axis, so that

$$C_{br} = C_{bt} C_{tr} \tag{3-2}$$

where C_{bt} is parameterized by Euler angles α_{bt} in a given sequence, and C_{tr} is an explicit function of time specifying the nominal attitude of the aircraft. The state equation in this coordinate patch becomes

$$\begin{aligned} \dot{r}_r &= v_r \\ \dot{v}_r &= C_{tr}^T f^f(u_m, u_p, u_f, \alpha_{bt}, v_t^a, \dot{\alpha}_{bt}, t) + g\delta_3 \\ \dot{(\alpha_{bt})} &= \dot{\alpha}_{bt} \\ \dot{(\dot{\alpha}_{bt})} &= \ddot{\alpha}_{bt} = f^\alpha(u_m, u_p, u_f, \alpha_{bt}, v_t^a, \dot{\alpha}_{bt}, t) \end{aligned} \tag{3-3}$$

The state space is flat. The force and moment functions (f^f, f^α) depend explicitly on time by virtue of the explicit time dependence of C_{tr}. Three derived functions are useful for control system design purposes. The first is the moment trim map, which will be defined as a partial inverse of f^α, and denoted by g^α:

$$\begin{aligned} u_m^c &= g^\alpha(\ddot{\alpha}_{bt}^c, u_p, u_f, \alpha_{bt}, v_t^a, \dot{\alpha}_{bt}, t) \\ \ddot{\alpha}_{bt}^c &= f^\alpha(u_m^c, u_p, u_f, \alpha_{bt}, v_t^a, \dot{\alpha}_{bt}, t) \end{aligned} \tag{3-4}$$

so that g^α computes the value u_m^c of the moment control that is required for the generation of a given Euler angle acceleration $\ddot{\alpha}_{bt}^c$, whereas all the other relevant variables are held fixed at some given values. The second is the force function subject to moment trim. It will be denoted by F^f and defined by the composite

$$F^f(\ddot{\alpha}_{bt}^c, u_p, u_f, \alpha_{bt}, v_t^a, \dot{\alpha}_{bt}, t) = f^f[g^\alpha(\ddot{\alpha}_{bt}^c, u_p, u_f, \alpha_{bt}, v_t^a, \dot{\alpha}_{bt}, t), u_p, u_f, \alpha_{bt}, v_t^a, \dot{\alpha}_{bt}, t] \tag{3-5}$$

The third derived function, denoted as F^α, is the force trim subject to moment trim. Here it will be defined implicitly as the solution to

$$F^f(\ddot{\alpha}_{bt}^c, u_p, u_f, \alpha_{bt}, v_t^a, \dot{\alpha}_{bt}, t) - f_t^c = 0 \tag{3-6}$$

The control mode defines how (u_p, u_f, α_{bt}) is to be partitioned into dependent and independent variables. For example, in the mode in which force is trimmed by means of roll, pitch, and thrust, the function F^α outputs the values of these variables for the given force f_t^c and all the remaining variables.

It may be noted that the selection of the coordinatization of the underlying state space and the selection of the control mode has a major effect on the form of the state equation. In addition, the output map h,

$$y = h(r_r, v_r, C_{br}, \omega_{brb}, u_p, u_f, w_r, C_{rt}) \tag{3-7}$$

is also defined by a mode—the output mode. Thus, for example, the output may be position r_r, or velocity v_r or its spherical or polar coordinates; or it may be the relative air velocity v_b^a, or perhaps aircraft attitude, C_{br}, or something else. Many output modes are of practical interest. The three types of modes, namely the mode that defines the coordinate patch, the mode that defines the flow of the control action through the system, and the mode that defines the output function, will be considered as components of a three-dimensional mode, which will be called the operation mode. Clearly, there are many values of the operation mode, and for each such mode there is a local state space model of the controlled process. The (possibly) multiaxis (multi-input multi-output) models have the following form.

$$\begin{aligned} \dot{x}_1 &= f_1(x_1, x_2, p) \\ \dot{x}_2 &= f_2(x_1, x_2, x_3, x_4, u, p) \\ \dot{x}_3 &= x_4 \\ \dot{x}_4 &= f_4(x_1, x_2, x_3, x_4, u, p) \\ y &= x_1 \end{aligned} \tag{3-8}$$

where $x_i, u \in R^m$, and $p \in R^k$ is a parameter, which is in general a given function of time. The state space is flat. The variables have been sorted out as follows.

(1) f_1 is invertible with respect to x_2,

$$\begin{aligned} x_2 &= g_1(x_1, \dot{x}_1, p) \\ f_1[x_1, g_1(x_1, \dot{x}_1, p), p] &= \dot{x}_1 \end{aligned} \tag{3-9}$$

(2) f_4 is invertible with respect to the moment control variable u. The moment trim map g^α in equation (3-4) will be denoted by

$$\begin{aligned} u &= g_4(x_1, x_2, x_3, x_4, u_2, p) \\ f_4[x_1, x_2, x_3, x_4, g_4(x_1, x_2, x_3, x_4, u_2, p), p] &= u_2 \end{aligned} \tag{3-10}$$

where u_2 is the desired moment $\dot{x}_4$. It may be considered as the new control variable.

(3) F_2 is the force function subject to moment trim.

$$F_2(x_1, x_2, x_3, x_4, u_2, p) = f_2[x_1, x_2, x_3, x_4, g_4(x_1, x_2, x_3, x_4, u_2, p), p] \tag{3-11}$$

This is F^f in equation (3-5). The functions g_4 and F_2 may be used to simplify the system in equation (3-8) as follows.

$$\begin{aligned} \dot{x}_1 &= f_1(x_1, x_2, p) \\ \dot{x}_2 &= F_2(x_1, x_2, x_3, x_4, u_2, p) \\ \dot{x}_3 &= x_4 \\ \dot{x}_4 &= u_2 \\ y &= x_1 \end{aligned} \tag{3-12}$$

In addition, we assume that F_2 is invertible with respect to x_3. This partial inverse will be denoted by

$$\begin{aligned} x_3 &= g_2(x_1, x_2, u_1, x_4, u_2, p) \\ F_2[x_1, x_2, g_2(x_1, x_2, u_1, x_4, u_2, p), x_4, u_2, p] &= u_1 \end{aligned} \tag{3-13}$$

where u_1 is interpreted as the desired acceleration $\dot{x}_2$.

(4) The output y is x_1, which will be interpreted as the generalized position of the aircraft, and x_2 and $\dot{x}_2$ as generalized velocity and acceleration, respectively.

The block diagram of the model is shown in figure 2. The presence of feed-forward is an indication of the presence of zero dynamics. If F_2 is independent of u_2 and x_4, then there is no feed-forward and no zero dynamics. This form will be referred to as pure feedback. If the model is in the pure feedback form, then the guidance trajectory can be obtained by inversion as follows. Suppose that the output y and its four time derivatives are given as functions of time, as are the parameter and its three time derivatives:

$$\begin{aligned} y_c^{[4]} &= \left(y_c^{(0)}, y_c^{(1)}, y_c^{(2)}, y_c^{(3)}, y_c^{(4)} \right) \\ p^{[3]} &= \left(p^{(0)}, p^{(1)}, p^{(2)}, p^{(3)} \right) \end{aligned} \tag{3-14}$$

Then, let

$$x_1^{[4]} = y_c^{[4]} \tag{3-15}$$

and obtain $x_2^{[3]}$ by computing

$$x_2 = g_1(x_1, x_1^{(1)}, p) \tag{3-16}$$

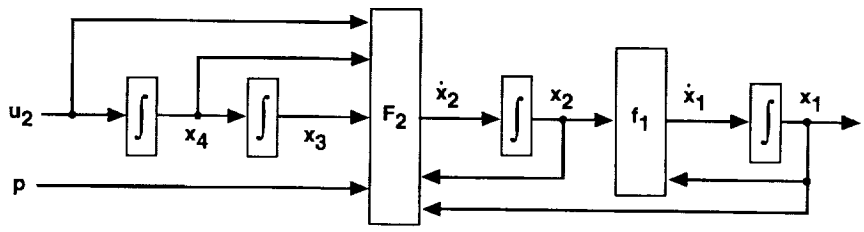

Figure 2. Local model of the controlled process.

and three of its time derivatives; then obtain $x_3^{[2]}$ by computing, with nulled-out zero dynamics,

$$x_3 = g_2(x_1, x_2, x_2^{(1)}, 0, 0, p) \tag{3-17}$$

and its two time derivatives, so that

$$\begin{aligned} x_4 &= x_3^{(1)} \\ u_2 &= x_3^{(2)} \\ u &= g_4(x_1, x_2, x_3, x_4, u_2, p) \end{aligned} \tag{3-18}$$

The resulting $x = (x_1, x_2, x_3, x_4)$ state and control u are then taken as the guidance state and control,

$$\begin{aligned} x^0 &= x \\ u^0 &= u \end{aligned} \tag{3-19}$$

The algorithm outlined above will be denoted as $\mathcal{F}_0$. In practice $\mathcal{F}_0$ is rather complicated. The basic force and moment functions (f_b^f, f_b^m) in equation (3-1) require many lines of code to implement. Many functions are involved—not only elementary functions such as sums, products, exponentials, and roots, but also multivariable polynomials, vector cross products, direction cosine matrices, and others. The functions are deeply nested in the sense of function-of-function evaluations. Furthermore, the transformation of (f_b^f, f_b^m) into (f_1, f_2, f_4) in equation (3-8) for a given operating mode requires further nonlinear computations such as the extraction of Euler angles from direction cosine matrices, the conversion of Cartesian coordinates into spherical, and other computations. Then it is necessary to obtain the inverses (g_1, g_2, g_4), and, finally, pass several time derivatives through them. The coding of $\mathcal{F}_0$ is very error prone. However, the application of dynamic forms as described in reference 7 simplifies the construction and coding of $\mathcal{F}_0$ from (f_b^f, f_b^m) to the level at which the inverison approach becomes quite tractable and error free. In the remainder of this report we assume that $\mathcal{F}_0$ is available.

Next, suppose that zero dynamics are present. Let the acceleration error be defined as follows:

$$\psi = F_2(x_1, x_2, x_3, x_4, u_2, p) - \dot{x}_2^0 \tag{3-20}$$

For the pure feedback solution the error in the command due to the ignored zero dynamics is then

$$\psi_0 = F_2(x_1^0, x_2^0, x_3^0, x_4^0, u_2^0, p) - \dot{x}_2^0 \tag{3-21}$$

A simple, practical way to control the effects of this error, if the zeros are weak, is to close a loop around it by means of a regulator as shown in figure 3. The guidance regulator (Greg) provides stable tracking. The plant model state and control are taken as the guidance command (x^g, u^g), which is executable in the sense that it is a stable solution of the system (eq. (3-8)). The guidance command serves as input to the real plant regulator (Preg), which closes the loop on the errors between x^g and the (estimated) real plant state x^p. In many practical cases this simple scheme works well. In the present report we are interested in cases in which the maneuvers are aggressive enough relative to the zero dynamics for this simple approach to be inadequate. The following example provides a simple illustration of such a case.

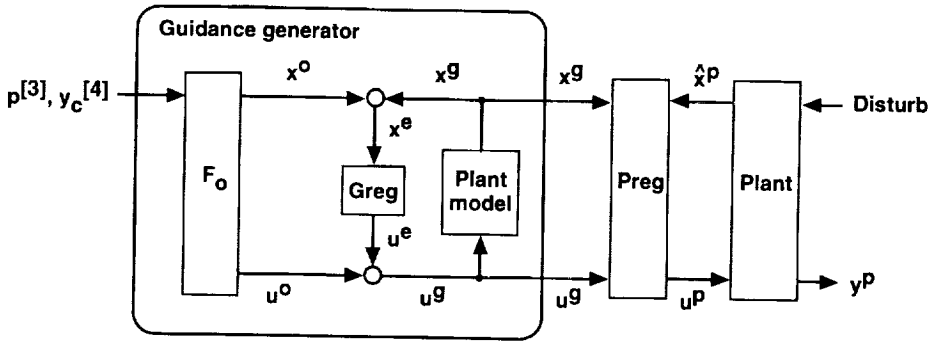

Figure 3. Structure of the guidance generator based on (x^0, u^0).

Linear Case

Consider a linear case of the system in equation (3-8):

$$\begin{aligned}
\dot{x}_1 &= x_2 \\
\dot{x}_2 &= f_2 = A_{21}x_1 + A_{22}x_2 + A_{23}x_3 + A_{24}x_4 + A_{25}u + A_{26}p \\
\dot{x}_3 &= x_4 \\
\dot{x}_4 &= f_4 = A_{41}x_1 + A_{42}x_2 + A_{43}x_3 + A_{44}x_4 + A_{45}u + A_{46}p \\
y &= x_1
\end{aligned} \tag{3-22}$$

We assume that A_{45} is not singular, and change control coordinates from u to u_2 (see eq. (3-10)):

$$u = g_4(x, u_2, p) = A_{45}^{-1}(u_2 - A_{41}x_1 - A_{42}x_2 - A_{43}x_3 - A_{44}x_4 - A_{46}p) \tag{3-23}$$

Then the state equation in new coordinates becomes

$$\begin{aligned}
\dot{x}_1 &= x_2 \\
\dot{x}_2 &= F_2 = C_1x_1 + C_2x_2 + C_3x_3 + C_4x_4 + C_5u_2 + C_6p \\
\dot{x}_3 &= x_4 \\
\dot{x}_4 &= u_2
\end{aligned} \tag{3-24}$$

where

$$\begin{aligned}
C_5 &= A_{25}A_{45}^{-1} \\
C_i &= A_{2i} - C_5A_{4i}
\end{aligned} \tag{3-25}$$

where $1 \leq i \leq 6$ and $i \neq 5$, and where u_2, the commanded angular acceleration, is the new directly accessible control variable. Equation (3-24) is the linear version of equation (3-12).

Next, assuming nonsingular C_3, the force trim map is given by the following (u_1 is the commanded $\dot{x}_2$):

$$x_3 = g_2 = C_3^{-1}(u_1 - C_1x_1 - C_2x_2 - C_4x_4 - C_5u_2 - C_6p) \tag{3-26}$$

The pure feedback solution (x^0, u_2^0) defined by equations (3-15) through (3-19) is given by

$$\begin{aligned} x_1^0 &= y_c \\ x_2^0 &= \dot{y}_c \\ x_3^0 &= C_3^{-1}(y_c^{(2)} - C_2 y_c^{(1)} - C_1 y_c^{(0)} - C_6 p^{(0)}) \\ x_4^0 &= C_3^{-1}(y_c^{(3)} - C_2 y_c^{(2)} - C_1 y_c^{(1)} - C_6 p^{(1)}) \\ u_2^0 &= C_3^{-1}(y_c^{(4)} - C_2 y_c^{(3)} - C_1 y_c^{(2)} - C_6 p^{(2)}) \end{aligned} \tag{3-27}$$

The corresponding acceleration error (eq. (3-21)) is

$$\psi_0 = C_4 C_3^{-1}(y_c^{(3)} - C_2 y_c^{(2)} - C_1 y_c^{(1)} - C_6 p^{(1)}) + C_5 C_3^{-1}(y_c^{(4)} - C_2 y_c^{(3)} - C_1 y_c^{(2)} - C_6 p^{(2)}) \tag{3-28}$$

Note that ψ_0 is continuous for small C_4 and C_5, and $\psi_0 = 0$ if C_4 and C_5 are both zero. We turn next to a numerical example.

Constant Linear Example – Part I

Suppose that the system (eq. (3-22)) is scalar, $x_i \in R^1$, $x \in R^4$, and

$$\begin{pmatrix} f_2 \\ f_4 \end{pmatrix} = \begin{pmatrix} 0.000 & -0.100 & 32.200 & 0.000 & -3.220 & 10.000 \\ 0.000 & -0.020 & -1.000 & -2.000 & 1.000 & -0.100 \end{pmatrix} \begin{pmatrix} x \\ u \\ p \end{pmatrix} \tag{3-29}$$

In our interpretation, one radian in x_3 generates one g acceleration $\dot{x}_2$, and $-0.1g$ is generated per unit of control u. After the inversion (eq. (3-10)), the force function in equation (3-11) becomes

$$F_2(x, u_2, p) = \begin{pmatrix} 0.000 & -0.164 & 28.980 & -6.440 & -3.220 & 9.678 \end{pmatrix} \begin{pmatrix} x \\ u_2 \\ p \end{pmatrix} \tag{3-30}$$

There are transmission zeros: translational acceleration $\dot{x}_2$ is affected by angular acceleration command u_2 at $-0.1g$/rad/sec^2.

We wish to transfer the system from hover at $y = 0$ to hover at $y = 1,000$ ft in 14 sec (from $t = 4$ to $t = 18$) as shown in figure 4, while changing the configuration parameter p from 0 to 1 and back to 0 as shown in the figure. The complete commanded maneuver y_c is composed of nine segments. Each segment is a 9-degree polynomial in t with continuous splices to order 4. The pure feedback solution (x^0, u_2^0) and the resulting acceleration error

$$\psi_0 = F_2(x^0, u_2^0, p) - \ddot{y}_c \tag{3-31}$$

caused by the zero dynamics are shown in figure 5. Errors of 9 ft/sec^2 are produced. We try to regulate the error by means of the plant model and regulator (Greg) structure shown in figure 3. A realistic regulator gain is

$$K = (\,0.0883 \quad 0.1354 \quad 6.8376 \quad 3.4005\,) \tag{3-32}$$

It places the two closed-loop pole pairs at 0.8 and 2 rad/sec, both with 0.5 damping. The resulting closed-loop error x^e response is shown in figure 6. The acceleration error produced by the zero dynamics results, in this case, in a tracking error x_1^e that reaches 11 ft. Furthermore, the regulator amplifies the closed-loop acceleration error ψ. We consider next a way for reducing the tracking error by providing a better guidance command (x^c, u^c). We will obtain an order-of-magnitude improvement (see fig. 13).

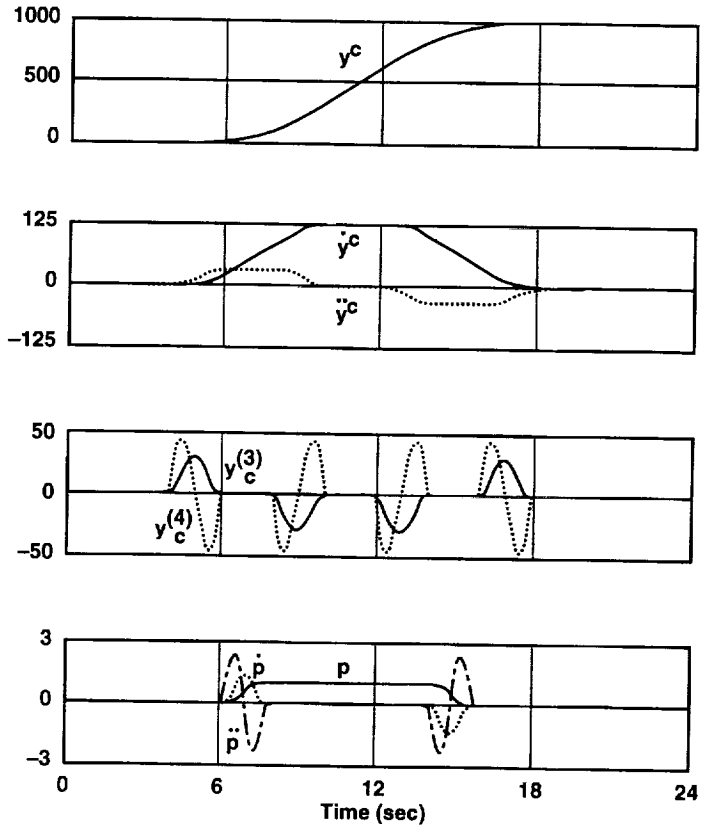

Figure 4. Commanded evolution of the output y and parameter p.

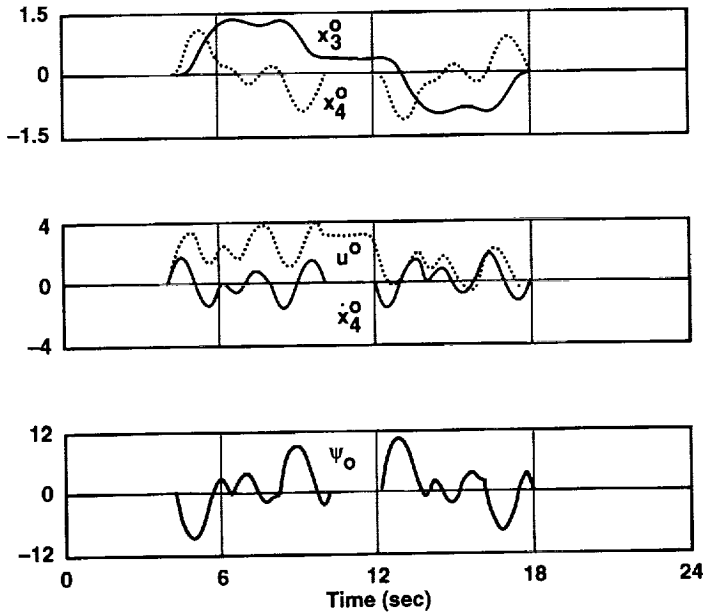

Figure 5. Pure feedback approximation and resulting error.

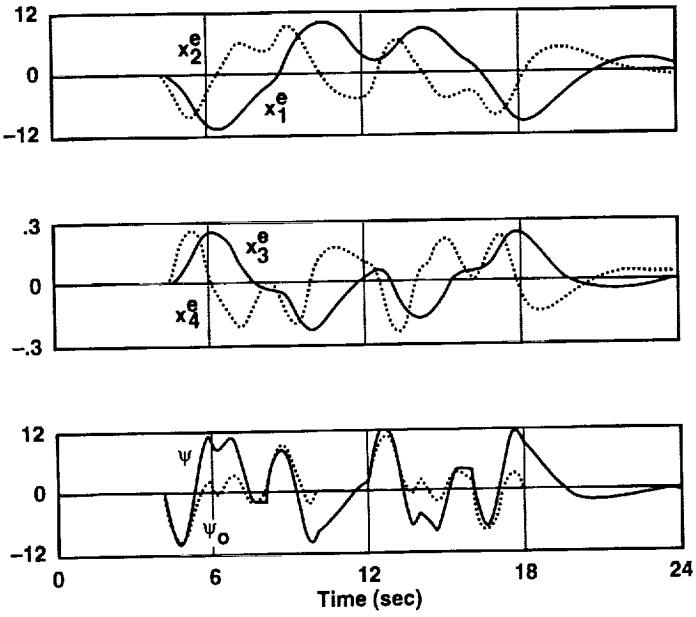

Figure 6. Error response.

4 Local Zero Dynamics

Let us return to the general case of the multiaxis system in equation (3-12). Suppose that in order to reduce the error ψ_0 defined by equation (3-21) we introduce perturbations (η_1, η_2, η_3) along the pure feedback solution (x^0, u_2^0). Then equation (3-20) becomes

$$\psi = F_2(x_1^0, x_2^0, x_3^0 + \eta_1, x_4^0 + \eta_2, u_2^0 + \eta_3, p) - \dot{x}_2^0 \tag{4-1}$$

or, using equation (3-21),

$$\psi = F_2(x_1^0, x_2^0, x_3^0 + \eta_1, x_4^0 + \eta_2, u_2^0 + \eta_3, p) - F_2(x_1^0, x_2^0, x_3^0, x_4^0, u_2^0, p) + \psi_0 \tag{4-2}$$

We assume that for small perturbations, the linear part dominates, so that (approximately)

$$\psi = C_3\eta_1 + C_4\eta_2 + C_5\eta_3 + \psi_0 \tag{4-3}$$

where the Jacobian matrices

$$\begin{aligned} C_3 &= \frac{\partial F_2}{\partial x_3} \\ C_4 &= \frac{\partial F_2}{\partial x_4} \\ C_5 &= \frac{\partial F_2}{\partial u_2} \end{aligned} \tag{4-4}$$

are evaluated along (x^0, u_2^0). We note that the Jacobian matrices can be computed directly from (f_2, f_4) in equation (3-8):

$$\begin{aligned} C_5 &= \frac{\partial f_2}{\partial u}\left(\frac{\partial f_4}{\partial u}\right)^{-1} \\ C_j &= \frac{\partial f_2}{\partial x_j} - C_5\frac{\partial f_4}{\partial x_j}, \quad j = 3, 4 \end{aligned} \tag{4-5}$$

If for each t in our interval of interest, $\mathcal{T} = [t_1, t_2]$, we select the perturbations (η_1, η_2, η_3) so that

$$C_3(t)\eta_1(t) + C_4(t)\eta_2(t) + C_5(t)\eta_3(t) = -\gamma\psi_0(t) \tag{4-6}$$

for $0 < \gamma \leq 1$, then we have improvement at each point of $\mathcal{T}$:

$$\psi(t) = (1 - \gamma)\psi_0(t) \tag{4-7}$$

The corresponding improved trajectory (x^1, u_2^1) is then

$$\begin{aligned} x_1^1 &= x_1^0 \\ x_2^1 &= x_2^0 \\ x_3^1 &= x_3^0 + \eta_1 \\ x_4^1 &= x_4^0 + \eta_2 \\ u_2^1 &= u_2^0 + \eta_3 \end{aligned} \tag{4-8}$$

and the improved error (eq. (3-20)) is

$$\psi_1 = F_2(x^1, u_2^1, p) - \dot{x}_2^0 \tag{4-9}$$

If the perturbations were free, we could have moved down in many ways, but of course the available perturbations are not free: according to equation (3-12) we have nonholonomic constraints, namely,

$$\begin{aligned} \dot{\eta}_1 &= \eta_2 \\ \dot{\eta}_2 &= \eta_3 \end{aligned} \tag{4-10}$$

so that, in fact, equation (4-6) is a differential equation,

$$C_5(t)\ddot{\eta} + C_4(t)\dot{\eta} + C_3(t)\eta = -\gamma\psi(t) \tag{4-11}$$

where $\eta = \eta_1$. If C_5 is nonsingular, then another form of this equation is given by

$$\ddot{\eta} + A_4(t)\dot{\eta} + A_3(t)\eta = B_2(t)[-\gamma\psi(t)] \tag{4-12}$$

or, equivalently,

$$\begin{pmatrix} \dot{\eta}_1 \\ \dot{\eta}_2 \end{pmatrix} = \begin{pmatrix} 0 & I \\ -A_3 & -A_4 \end{pmatrix} \begin{pmatrix} \eta_1 \\ \eta_2 \end{pmatrix} + \begin{pmatrix} 0 \\ B_2 \end{pmatrix} (-\gamma\psi) \tag{4-13}$$

where, of course, $B_2 = C_5^{-1}$, $A_4 = B_2 C_4$, and $A_3 = B_2 C_3$, that is,

$$\begin{aligned} B_2 &= \frac{\partial f_4}{\partial u}\left(\frac{\partial f_2}{\partial u}\right)^{-1} \\ A_j &= B_2 \frac{\partial f_2}{\partial x_j} - \frac{\partial f_4}{\partial x_j}, \quad j = 3, 4 \end{aligned} \tag{4-14}$$

We will refer to all three forms of the differential equation as the local zero dynamics (of the system in eq. (3-12)). We seek the stable, "steady state" solution of the local zero dynamics. We develop methods for the computation of such solutions in the next two sections, first using the time domain approach and then using the frequency domain approach. Assuming that the steady state solution can be computed, the proposed algorithm for the computation of the improved guidance command (x^c, u_2^c) can be summarized as follows.

Step 1. Compute the pure feedback solution (x^0, u_2^0) and the error ψ_0.

Step 2. Compute the Jacobian matrices C_3, C_4, and C_5 along (x^0, u_2^0).

Step 3. Compute the steady state solution of the local zero dynamics.

Step 4. Update the trajectory and compute the improved error ψ.

Step 5. Repeat steps 2–4 until $|\psi|$ becomes acceptable; the result is (x^c, u_2^c).

If the system (eq. (3-8)) is linear, a choice of $\gamma = 1$ will produce the result in one iteration. Otherwise, γ must be small enough for the linear part of the perturbation to be dominant. The effect of nonlinearity is to increase the number of required iterations.

The differential equation (4-11) is closely related to the Isidori zero dynamics (ref. 8), which for the system (eq. (3-12)) are defined by the generally nonlinear differential equation

$$F_2(x_1^0, x_2^0, z, \dot{z}, \ddot{z}, p) = \dot{x}_2^0 \tag{4-15}$$

Let $z(t)$ be its stable, steady state solution. The linear part of the perturbation along $z(t)$ is given by

$$C_5(t)\ddot{\eta} + C_4(t)\dot{\eta} + C_3(t)\eta = \psi(t) \tag{4-16}$$

where the Jacobian matrices C_i are evaluated along $z(t)$. Thus, the homogeneous parts of equations (4-11) and (4-16) are the same for perturbations along $z(t)$, but unless F_2 is linear the Jacobian matrices will be different in the early stages of our iteration.

There are three approaches to solving the differential equation (4-15).

(1) In reference 3 the approach is to represent the command y_c and the parameter p as outputs of a relaxing exosystem, and then to design a regulator that forces the combined system to satisfy equation (4-15) asymptotically.

(2) In reference 6 the approach is to solve equation (4-15) by means of a Picard-like iteration.

(3) Our approach is to solve equation (4-15) by replacing it with a sequence of linear problems; each linear problem is solved by means of a Picard-like iteration (ref. 6). The advantage of this approach is the freedom provided by γ: it controls the intensity of the forcing function $\gamma\psi$.

Approaches (2) and (3) are distinct only for nonlinear systems. For linear systems they are the same.

The remaining problem is to develop a procedure to carry out step 3 in the above algorithm. For the case of our numerical example in equation (3-29), this requires finding the particular solution of the following differential equation.

$$-3.220\ddot{\eta} - 6.440\dot{\eta} + 28.980\eta = -\psi_0 \tag{4-17}$$

Its eigenvalues $(\lambda_1, \lambda_2) = (-4.162, 2.162)$. There is a nonminimum phase zero at 2.162. In order to reduce the errors shown in figures 5 and 6, we need the steady state solution of this equation. That type of problem is solved next. We follow the procedure given in reference 6.

5 Time Domain Solution of the Local Zero Dynamics

Consider the constant linear system

$$\dot{x} = Ax + Bu \tag{5-1}$$

where $x \in R^n$, $u \in R^m$, and A has no eigenvalues on the $j\omega$ axis. We are not interested in the usual initial value problem in which $x(0)$ and u are given and the problem is to find the solution $x(t)$. Instead, we want to compute the particular solution x_p for a given u. For example, what is the constant x for a given constant u, or what is the amplitude and phase of x for a given sinusoidal u, or what is x for an arbitrary given u? The answers to the first two questions are easy:

$$x_p(j\omega) = (j\omega I - A)^{-1} B u(j\omega) \tag{5-2}$$

The third question is addressed in the rest of this section and in the next section.

Constant Linear Systems

Assume for simplicity that A has distinct eigenvalues. Change coordinates

$$x = Pz \tag{5-3}$$

to diagonalize A

$$P^{-1}AP = \Lambda \tag{5-4}$$

so that

$$\dot{z} = \Lambda z + \Gamma u \tag{5-5}$$

where $\Gamma = P^{-1}B$. The transition matrix for this system, which is diagonal, we separate into stable and unstable parts, $\varphi^-(t)$ and $\varphi^+(t)$, respectively:

$$\varphi(t) = e^{\Lambda t} = \varphi^-(t) + \varphi^+(t) \tag{5-6}$$

The bilateral (ref. 6) transition matrix for equation (5-5) is then given by

$$\varphi^{\pm}(t) = \varphi^-(t)U(t) - \varphi^+(t)U(-t) \tag{5-7}$$

where U is the unit step function. The particular solution is given by the convolution

$$z_p(t) = \int_{-\infty}^{+\infty} \varphi^{\pm}(t-\tau)\Gamma u(\tau) d\tau \tag{5-8}$$

That z_p is a solution of equation (5-5) can be checked by differentiation. Note that $\varphi^-(0)+\varphi^+(0) = I$, and that φ^- and φ^+ cannot have nonzero entries in the same row.

By transforming back to the natural coordinates, we obtain the bilateral transition matrix

$$\phi^{\pm}(t) = P\varphi^{\pm}(t)P^{-1} \tag{5-9}$$

and the bilateral input-output impulse response

$$h^{\pm}(t) = P\varphi^{\pm}(t)P^{-1}B \tag{5-10}$$

The particular solution to equation (5-1) is given by the convolution

$$x_p(t) = \int_{-\infty}^{+\infty} h^{\pm}(t-\tau)u(\tau)d\tau \tag{5-11}$$

or, equivalently, the computationally more convenient form

$$x_p(t) = \int_{-\infty}^{+\infty} h^{\pm}(-\sigma)u(t+\sigma)d\sigma \tag{5-12}$$

In the present report we are interested in the second-order system given by equation (4-13). Application of equation (5-12) with $u = -\gamma\psi$ produces the following particular solution:

$$\begin{pmatrix} \eta_1(t) \\ \eta_2(t) \end{pmatrix} = -\gamma \int_{-\infty}^{+\infty} h^{\pm}(-\sigma)\psi(t+\sigma)d\sigma \tag{5-13}$$

For the scalar case,

$$\ddot{\eta} + a_4\dot{\eta} + a_3\eta = b_2 \cdot (-\gamma\psi) \tag{5-14}$$

$$A = \begin{pmatrix} 0 & 1 \\ -a_3 & -a_4 \end{pmatrix}, \; B = \begin{pmatrix} 0 \\ b_2 \end{pmatrix} \tag{5-15}$$

with $\lambda_1 < 0 < \lambda_2$

$$P = \begin{pmatrix} 1 & 1 \\ \lambda_1 & \lambda_2 \end{pmatrix}, \quad P^{-1} = \frac{1}{\lambda_2 - \lambda_1}\begin{pmatrix} \lambda_2 & -1 \\ -\lambda_1 & 1 \end{pmatrix} \tag{5-16}$$

so that

$$\varphi^{-}(t) = \begin{pmatrix} e^{\lambda_1 t} & 0 \\ 0 & 0 \end{pmatrix}, \quad \varphi^{+}(t) = \begin{pmatrix} 0 & 0 \\ 0 & e^{\lambda_2 t} \end{pmatrix} \tag{5-17}$$

and

$$h^{\pm}(t) = -\frac{b_2}{\lambda_2 - \lambda_1}\left[\begin{pmatrix} 1 \\ \lambda_1 \end{pmatrix} e^{\lambda_1 t}U(t) + \begin{pmatrix} 1 \\ \lambda_2 \end{pmatrix} e^{\lambda_2 t}U(-t)\right] \tag{5-18}$$

The first component of $h^{\pm}(t)$,

$$h_1^{\pm}(t) = -\frac{b_2}{\lambda_2 - \lambda_1}[e^{\lambda_1 t}U(t) + e^{\lambda_2 t}U(-t)] \tag{5-19}$$

is shown in figure 7 for the case of equation (4-17), where $(\lambda_1, \lambda_2) = (-4.162, 2.162)$. Note the rapid roll-off on either side of $t = 0$. One may expect that, for reasonable forcing functions $-\gamma\psi$, the convolution may be restricted to, say, only four times the slowest time constant, which in the case shown is approximately 2 sec.

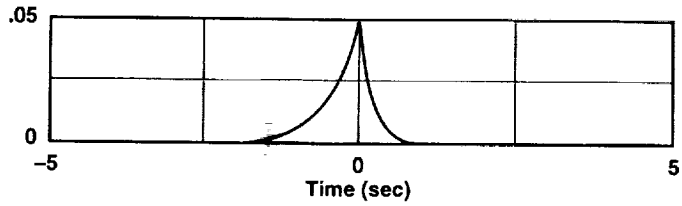

Figure 7. Numerical example of $h_1^{\pm}(t)$.

If we define

$$\begin{aligned} \mu_1(t) &= \int_{-\infty}^{t} e^{\lambda_1(t-\tau)} u(\tau) d\tau \\ \mu_2(t) &= \int_{t}^{+\infty} e^{\lambda_2(t-\tau)} u(\tau) d\tau \end{aligned} \tag{5-20}$$

then the particular solution of equation (5-14) is given by

$$\begin{aligned} \eta(t) &= \tfrac{b_2\gamma}{\lambda_2-\lambda_1}[\mu_1(t) + \mu_2(t)] \\ \dot{\eta}(t) &= \tfrac{b_2\gamma}{\lambda_2-\lambda_1}[\lambda_1\mu_1(t) + \lambda_2\mu_2(t)] \\ \ddot{\eta}(t) &= -a_3\eta(t) - a_4\dot{\eta}(t) - b_2\gamma\psi(t) \end{aligned} \tag{5-21}$$

In order to explore this solution, suppose that we have a table of integrals so that for a given ψ,

$$\int e^{\lambda t}\psi(t)dt = \Psi(\lambda, t), \quad \dot{\Psi}(\lambda, t) = e^{\lambda t}\psi(t) \tag{5-22}$$

Then

$$\begin{aligned} \mu_1(t) &= e^{\lambda_1 t}\Psi(-\lambda_1, t) \\ \mu_2(t) &= -e^{\lambda_2 t}\Psi(-\lambda_2, t) \end{aligned} \tag{5-23}$$

If $\psi(t) = 1$, then $\Psi(\lambda, t) = e^{\lambda}/\lambda$, and

$$\begin{aligned} \mu_1 &= \tfrac{-1}{\lambda_1} \\ \mu_2 &= \tfrac{1}{\lambda_2} \end{aligned} \tag{5-24}$$

so that the particular solution is, as expected from equation (5-14),

$$\begin{aligned} \eta &= \tfrac{b_2\gamma}{\lambda_1\lambda_2} = \tfrac{-b_2\gamma}{a_3} \\ \dot{\eta} &= 0 \\ \ddot{\eta}_2 &= 0 \end{aligned} \tag{5-25}$$

If $\psi(t) = \sin(\omega t)$, then

$$\begin{aligned}\mu_1 &= e^{\lambda_1 t}\Psi(-\lambda_1, t) = \tfrac{1}{\lambda_1^2+\omega^2}[-\lambda_1 \sin(\omega t) - \omega\cos(\omega t)] \\ \mu_2 &= -e^{\lambda_2 t}\Psi(-\lambda_2, t) = \tfrac{-1}{\lambda_2^2+\omega^2}[-\lambda_2 \sin(\omega t) - \omega\cos(\omega t)]\end{aligned} \tag{5-26}$$

so that

$$\eta = -\gamma a \sin(\omega t + \theta) \tag{5-27}$$

where

$$a e^{j\theta} = \frac{b_2}{-\omega^2 + j\omega a_4 + a_3} \tag{5-28}$$

Discontinuities in ψ or its derivatives spawn leading (noncausal) and trailing transients. For example, consider a pulse,

$$\psi(t) = \begin{cases} 0, & t < t_1 \\ \psi_0(t), & t_1 < t < t_2 \\ 0, & t_2 < t \end{cases} \tag{5-29}$$

Then

$$\mu_1 = \begin{cases} 0, & t < t_1 \\ e^{\lambda_1 t}[\Psi_0(-\lambda_1, t) - \Psi_0(-\lambda_1, t_1)], & t_1 < t < t_2 \\ e^{\lambda_1 t}[\Psi_0(-\lambda_1, t_2) - \Psi_0(-\lambda_1, t_1)], & t_2 < t \end{cases} \tag{5-30}$$

and

$$\mu_2 = \begin{cases} e^{\lambda_2 t}[\Psi_0(-\lambda_2, t_2) - \Psi_0(-\lambda_2, t_1)], & t < t_1 \\ e^{\lambda_2 t}[\Psi_0(-\lambda_2, t_2) - \Psi_0(-\lambda_2, t)], & t_1 < t < t_2 \\ 0, & t_2 < t \end{cases} \tag{5-31}$$

That is, there is a pair of transients at either end of the pulse. One member of the pair leads the discontinuity, the other trails it. For example, suppose that

$$\psi(t) = \begin{cases} 0, & t < 0 \\ 1 - \cos(\omega t), & 0 < t < t_2 = \frac{2\pi}{\omega} \\ 0, & t_2 < t \end{cases} \tag{5-32}$$

One way to get the particular solution is to splice three segments of particular solutions,

$$\eta(t) = \begin{cases} 0, & t < 0 \\ a_0 - a\cos(\omega t + \theta), & 0 < t < t_2 \\ 0, & t_2 < t \end{cases} \tag{5-33}$$

where $a_0 = -b_2\gamma/a_3$, and a and θ are given by equation (5-28). But that simple approach produces undesirable discontinuities in η and $\dot{\eta}$ at $t = 0$ and $t = t_2$. On the other hand, the particular solution

$$\eta(t) = \frac{-b_2\gamma}{\lambda_2 - \lambda_1}[\mu_1(t) + \mu_2(t)] \tag{5-34}$$

and its derivative are everywhere continuous. The leading and trailing transients satisfy the homogeneous part

$$\ddot{\eta} + a_4\dot{\eta} + a_3\eta = 0 \tag{5-35}$$

These transients prepare the system state x and control u for the approaching discontinuity, and the transients are invisible at the system output y. Thus, the bilateral solution has definite advantages.

Numerical Solution

Numerical solutions of the convolution integrals are needed in practical applications. The integrals in equation (5-20) may be computed approximately as follows.

$$\begin{aligned}
\mu_1 &= e^{\lambda_1 t}\int_{-\infty}^{t} e^{-\lambda_1\tau}\psi(\tau)d\tau = \sum_{n=0}^{\infty}\int_{t-nT-T}^{t-nT} e^{-\lambda_1\tau}\psi(\tau)d\tau \approx \\
\mu_1^* &= \frac{1-e^{\lambda_1 T}}{-\lambda_1(1-e^{\lambda_1 TN})}\sum_{n=0}^{N}(e^{\lambda_1 T})^n[\psi(t-nT-T)+\psi(t-nT)]/2 \\
\mu_2 &= e^{\lambda_2 t}\int_{t}^{\infty} e^{-\lambda_2\tau}\psi(\tau)d\tau = \sum_{n=0}^{\infty}\int_{t+nT+T}^{t+nT} e^{-\lambda_2\tau}\psi(\tau)d\tau \approx \\
\mu_2^* &= \frac{1-e^{-\lambda_2 T}}{\lambda_2(1-e^{-\lambda_2 TN})}\sum_{n=0}^{N}(e^{-\lambda_2 T})^n[\psi(t+nT+T)+\psi(t+nT)]/2
\end{aligned} \tag{5-36}$$

The approximations have been normalized to give correct results for $\psi = 1$. Consequently, the approximate solution to our problem is given by

$$\begin{aligned}
\eta_1^* &= \frac{b_2}{\lambda_2-\lambda_1}(\mu_1^*+\mu_2^*) \\
\eta_2^* &= \frac{b_2}{\lambda_2-\lambda_1}(\lambda_1\mu_1^*+\lambda_2\mu_2^*) \\
\eta_3^* &= -a_3\eta_1^* - a_4\eta_2^* - b_2\gamma\psi(t)
\end{aligned} \tag{5-37}$$

For example, consider yet again the system discussed previously,

$$\begin{aligned}
(a_3, a_4, b) &= (-9.000 \quad 2.000 \quad 0.311) \\
(\lambda_1, \lambda_2) &= (-4.162 \quad 2.162)
\end{aligned} \tag{5-38}$$

Assume that the forcing function is

$$(-\gamma\psi) = 20\sin(\omega t + \pi/4) \tag{5-39}$$

so that the exact solution is easily obtained as the particular solution:

$$\eta(j\omega) = \frac{-0.311}{(-\omega^2 + j\omega 2 - 9)}\psi(j\omega) \tag{5-40}$$

We take the sampling period $T = 0.05$ sec and provide a look-ahead/look-back of $N = 40$ samples (± 2 sec). The approximate computation $\eta^*(0)$ is compared to the exact $\eta(0)$ for several frequencies. A frequency scan from $[0, 10]$ rad/sec is shown figure 8. The approximate and exact solutions are practically indistinguishable in the figure. Hence this type of algorithm is effective for constant systems. We now turn to the time-varying case.

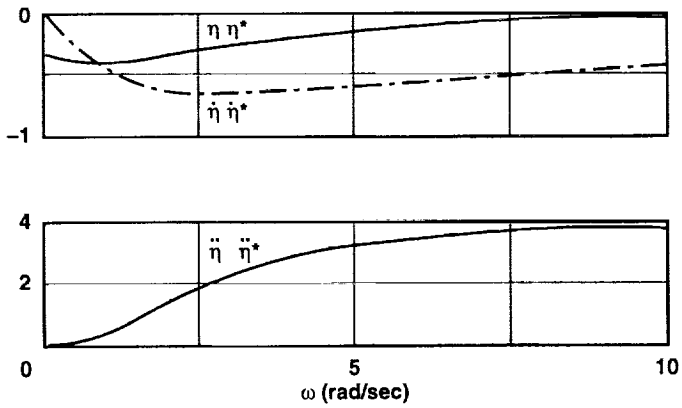

Figure 8. Exact and approximate solutions.

Linear Time-Varying Systems

In general, the local zero dynamics given by equation (4-13) may have time-varying coefficients. Therefore, consider the following model

$$\dot{x} = [A_0 + \delta A(t)]x + B(t)u(t) \tag{5-41}$$

where $x \in R^n$, $u \in R^m$, and δA and B are some reasonable functions of time. The iteration in reference 6, restricted to linear systems, will converge to the particular solution if the following conditions hold:

(1) A_0 has no eigenvalues on the $j\omega$ axis; $\phi^{\pm}(t)$ is the bilateral solution for the system

$$\dot{x} = A_0 x \tag{5-42}$$

and let the norm of $\phi^{\pm}$ be

$$\|\phi^{\pm}\| = \sum_j \max_k \int_{-\infty}^{\infty} |\phi^{\pm}_{jk}(t)|dt \tag{5-43}$$

(2) There is a constant K so that for all $-\infty < t < \infty$

$$\max_{i,j} |\delta a_{ij}(t)| \leq K \tag{5-44}$$

(3) The product

$$K\|\phi^{\pm}\| < 1 \tag{5-45}$$

The solution is constructed by means of a Picard-like iteration:

$$\begin{aligned} x_0(t) &\equiv 0 \\ x_1(t) &= \int_{-\infty}^{\infty} \phi^{\pm}(t-\tau)B(\tau)u(\tau)d\tau \\ x_{m+1}(t) &= x_1(t) + \int_{-\infty}^{\infty} \phi^{\pm}(t-\tau)\delta A(\tau)x_m(\tau)d\tau \end{aligned} \tag{5-46}$$

The difference at each iteration

$$\begin{aligned} e_m(t) &= x_{m+1}(t) - x_m(t) = \int_{-\infty}^{\infty} \phi^{\pm}(t-\tau)\delta A(\tau)e_{m-1}(\tau)d\tau \\ \max_t \|e_m(t)\| &\leq \max_t \|x_1(t)\|(K\|\phi^{\pm}\|)^m \end{aligned} \tag{5-47}$$

so that

$$x_p(t) = \lim_{m\to\infty} x_m(t) \tag{5-48}$$

In actual applications, it may be advantageous to change coordinates. For example, suppose that A_0 has only real and distinct eigenvalues, and that P diagonalizes it. Then

$$\|\varphi^{\pm}\| = \sum \frac{1}{|\lambda_i|} = \sum \tau_i \tag{5-49}$$

that is, the sum of time constants, and condition (3) becomes

$$K\sum \tau_i < 1 \tag{5-50}$$

In the scalar case of equation (4-12), separate the time variation as follows

$$\ddot{\eta} + [a_{04} + \delta a_4(t)]\dot{\eta} + [a_{03} + \delta a_3(t)]\eta = -b_2(t)\gamma\psi(t) \tag{5-51}$$

If the eigenvalues of A_0 satisfy $\lambda_1 < 0 < \lambda_2$, and if for $-\infty < t < \infty$

$$\max[|\delta a_3(t)|, |\delta a_4(t)|](\tau_1 + \tau_2) < 1 \tag{5-52}$$

then the iteration will converge to the particular solution.

In summary, if the coefficients of the local zero dynamics vary in time sufficiently little relative to their average value, then the iteration will produce the particular solution, and so step 3 in our algorithm can be carried out. The overall algorithm is thus complete. The time domain approach seems to require a lot of bookkeeping with respect to the eigenvalue pattern. The frequency domain approach discussed next is simpler, especially for multiaxes systems.

6 Frequency Domain Solution of the Local Zero Dynamics

Consider again the local zero dynamics (eq. (4-11))

$$C_5(t)\ddot{\eta} + C_4(t)\dot{\eta} + C_3(t)\eta = -\gamma\psi(t) \tag{6-1}$$

We are interested in obtaining the particular solution. In the preceding section, we took the time domain approach, which has some drawbacks. The need to distinguish between root patterns is a nuisance. Also, we would like to consider cases where C_5 drifts through zero, which leads to changing order of the differential equation. The frequency domain approach, discussed next, is in some ways much simpler to implement.

Let us rewrite equation (6-1) as a sum of constant and time-varying linear operators

$$(L_0 + \delta L)\eta = -\gamma\psi \tag{6-2}$$

where $D = d/dt$ and

$$\begin{aligned} L_0 &= C_5^0 D^2 + C_4^0 D + C_3^0 \\ \delta L &= \delta C_5(t) D^2 + \delta C_4(t) D + \delta C_3(t) \end{aligned} \tag{6-3}$$

Let η_0 be the solution of the time invariant part

$$\eta_0 = L_0^{-1}(-\gamma\psi) \tag{6-4}$$

and change coordinates so that $\eta = \eta_0 + \eta_1$. Then

$$(L_0 + \delta L)(\eta_0 + \eta_1) = -\gamma\psi \tag{6-5}$$

That is,

$$(L_0 + \delta L)\eta_1 = -\delta L \eta_0 \tag{6-6}$$

This is the old equation (6-2) with a new forcing term, which is the error caused by η_0. After i iterations, the correction is

$$\eta_{i+1} = -L_0^{-1}\delta L \eta_i \tag{6-7}$$

If $\|L_0^{-1}\delta L\| < 1$, then the iterations

$$\eta = \sum \eta_i \tag{6-8}$$

converge to the solution of equation (6-2) and hence of the original equation (6-1). Consider next the construction of L_0^{-1}.

The Fourier transform of equation (6-4) is

$$\eta_0(j\omega) = G_0(j\omega)[-\gamma\psi(j\omega)] \tag{6-9}$$

where the transfer function

$$G_0(j\omega) = [C_5^0(j\omega)^2 + C_4^0 j\omega + C_3^0]^{-1} \tag{6-10}$$

The forcing function $\psi(t)$ is available only at sampling points, $\psi(nT)$. The Shannon reconstruction (ref. 9), with $sinc(x) = sin(x)/x$,

$$\psi(t) = T \sum_{-\infty}^{+\infty} \psi(nT) sinc[\omega_s(t - nT)/2]/T \tag{6-11}$$

converts the sequence $\psi(nT)$ into an analog signal, $\psi(t)$, that is band-limited to $|\omega| \leq \omega_s/2 = \pi/T$. The Fourier transform of $sinc(\omega_s t/2)/T$ is

$$S(j\omega) = \begin{cases} 1, & |\omega| \leq \omega_s/2 \\ 0, & |\omega| > \omega_s/2 \end{cases} \tag{6-12}$$

Hence, the transform of the output of G_0 with input $sinc(\omega_s t/2)/T$ is

$$g_0(j\omega) = G_0(j\omega)S(j\omega) \tag{6-13}$$

and its inverse is

$$g_0(t) = \tfrac{1}{2\pi} \textstyle\int_{-\omega_s/2}^{+\omega_s/2} G_0(j\omega) e^{j\omega t} d\omega \tag{6-14}$$

or, equivalently, because of symmetries,

$$g_0(t) = \frac{1}{\pi} \int_0^{\omega_s/2} (G_{0x} \cos \omega t - G_{0y} \sin \omega t) d\omega \tag{6-15}$$

where G_{0x} and G_{0y} are, respectively, the real and imaginary parts of G_0. The integral is then computed numerically (we used an IMSL, Inc., routine (ref. 10)) for $2N_s + 1$ values of t to obtain the sequence

$$\{g_0(kT),\ -N_s \leq k \leq N_s\} \tag{6-16}$$

Then, finally, the frequency domain approximation η^ω to the particular solution of equation (6-4) is given by the following discrete convolution:

$$\eta^\omega(nT) = -\gamma T \sum_{k=-N_s}^{N_s} \psi[(n-k)T)] g_0(kT) \tag{6-17}$$

The derivatives $\dot{\eta}^\omega$ and $\ddot{\eta}^\omega$ are computed similarly by means of equation (6-17), except that g_0 is replaced by g_1 and g_2, which are the inverse transforms of $G_1(j\omega) = j\omega G_0(j\omega)$ and $G_2(j\omega) = (j\omega)^2 G_0(j\omega)$, respectively.

The potential aliasing problem arising from the multiplication in forming $\delta L \eta_i$ may be avoided by means of a noncausal filter G_f, which provides roll-off without phase lag. In that case the combined transfer function

$$G_0(j\omega) = [C_5^0(j\omega)^2 + C_4^0 j\omega + C_3^0]^{-1} G_f(j\omega) \tag{6-18}$$

where $G_f(s)$ is symmetric about both real and imaginary axes. For example, if, as before, $(c_5, c_4, c_3) = (-3.22, -6.44, 28.98)$, we may choose

$$G_0(j\omega) = [-3.22(j\omega)^2 - 6.44(j\omega) + 28.98]^{-1} [1 + (\omega/8)^4]^{-1} \tag{6-19}$$

The response g_0 of the (unstable) G_0 to $sinc(\omega_s t/2)/T$ is shown in figure 9. Also shown is the corresponding bilateral impulse response $h_1^{\pm}$ (see fig. 7). It may be noted that the two curves are practically indistinguishable, which is not surprising since $h_1^{\pm}(t)$ and $G_0(j\omega)$ (without the filter) are a Fourier transform pair.

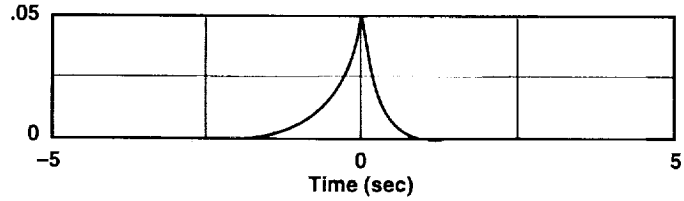

Figure 9. Comparison of $h_1^{\pm}$ with the response g_0 of G_0 to $sinc(w_s t/2)/T$.

Thus we have two effective ways for computing the steady state solution of the local zero dynamics. One solves the problem in time domain producing the approximation η^*; the other solves the problem in frequency domain producing the approximation η^{ω}.

7 Outline of the Proposed Algorithm

An approach has been presented in this report for the computation of the guidance commands (x^c, u^c) that guide the system along y_c. The system may be multiaxis, time-varying, and nonlinear, but of the following type (see eq. (3-8))

$$\begin{aligned} \dot{x}_1 &= f_1(x_1, x_2, p) \\ \dot{x}_2 &= f_2(x_1, x_2, x_3, x_4, u, p) \\ \dot{x}_3 &= x_4 \\ \dot{x}_4 &= f_4(x_1, x_2, x_3, x_4, u, p) \\ y &= x_1 \end{aligned} \tag{7-1}$$

where $x_i, u \in R^m$ and $p \in R^k$ is a time-dependent parameter. This is a realistic model of an aircraft. The algorithm consists of the following steps.

Step 1. Change the control variable to $u_2 = f_4(x_1, x_2, x_3, x_4, u, p)$ so that the model becomes

$$\begin{aligned} \dot{x}_1 &= f_1(x_1, x_2, p) \\ \dot{x}_2 &= F_2(x_1, x_2, x_3, x_4, u_2, p) \\ \dot{x}_3 &= x_4 \\ \dot{x}_4 &= u_2 \\ y &= x_1 \end{aligned} \tag{7-2}$$

Step 2. Initialize $(i = 0)$ the following iteration by inverting the pure feedback part of the system,

$$\begin{aligned} x_1^i &= y_c \\ x_2^i &= g_1(x_1^i, \dot{x}_1^i, p) \\ x_3^i &= g_2(x_1^i, x_2^i, \dot{x}_2^i, 0, 0, p) \\ x_4^i &= \dot{x}_3^i \\ u_2^i &= \dot{x}_4^i \end{aligned} \tag{7-3}$$

Step 3. Compute the error in $\dot{x}_2$ caused by the neglected dynamics:

$$\psi_i = F_2(x_1^i, x_2^i, x_3^i, x_4^i, u_2^i, p) - \dot{x}_2^0 \tag{7-4}$$

Skip Steps 4–6 if $|\psi_i|$ is small enough.

Step 4. Compute the Jacobian matrices C_3^i, C_4^i, and C_5^i along (x^i, u_2^i).

Step 5. Compute iteratively the particular solution of the local zero dynamics,

$$C_5^i \ddot{\eta} + C_4^i \dot{\eta} + C_3^i \eta = -\gamma \psi_i \tag{7-5}$$

Step 6. Update trajectory (x^i, u_2^i)

$$\begin{aligned} x_1^{i+1} &= x_1^0 \\ x_2^{i+1} &= x_2^0 \\ x_3^{i+1} &= x_3^i + \eta \\ x_1^{i+1} &= x_4^i + \dot{\eta} \\ u_2^{i+1} &= u_2^i + \ddot{\eta} \end{aligned} \tag{7-6}$$

Step 7. Compute the control in natural coordinates

$$u^i = g_4(x_1^i, x_2^i, x_3^i, x_4^i, u_2^i, p) \tag{7-7}$$

The result is the guidance trajectory (x^c, u^c), which includes the effects of zero dynamics. For linear systems one iteration with $\gamma = 1$ will suffice. For nonlinear systems, γ is chosen small enough to ensure the dominance of the linear approximation. If many iterations are needed in a given problem, then the accumulation of small errors may make the iterate (x_3^i, x_4^i, u_2^i) inconsistent with the nonholonomic constraints,

$$\begin{aligned} \dot{x}_3^i &= x_4^i \\ \dot{x}_4^i &= u_2^i \end{aligned} \tag{7-8}$$

That can be easily rectified by passing each iterate through a noncausal observer for the constraint (eq. (7-8)).

The resulting structure of the command generator shown in figure 10 is the same as in figure 3, except that the pure feedback guidance (x^0, u^0), which does not account for zero dynamics, is replaced by (x^c, u^c), which does. We now apply, by way of illustration, the complete algorithm to compute the guidance command (x^c, u^c) for several examples.

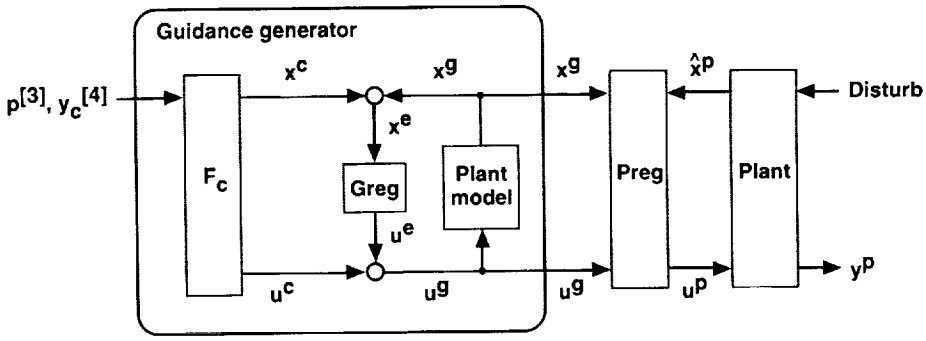

Figure 10. Structure of the guidance generator based on (x^c, u^c).

8 Examples

In this section we apply the numerical solution of the local zero condition to the linear model discussed previously and describe the resulting closed-loop behavior. Later in this section, we apply the proposed guidance method to a time-varying system, and then to a nonlinear system.

Constant Linear Example – Part II

In the first part of this example (see Constant Linear Example – Part I) we have computed and stored in memory the error $\psi_0(t)$ on the time interval $[0, 26]$ at 20 samples per sec. Now we pass this sequence $\psi_0(nT)$ with $\gamma = 1$ through the algorithm (eqs. (5-36) and (5-37)), 81 samples ($N = 40$) at a time at each sample, to obtain the corrections $(\eta^*, \dot{\eta}^*, \ddot{\eta}^*)$. The first panel of figure 11 shows both time domain η^* and frequency domain η^ω (with $N_s = 40$) solutions. They are indistinguishable. The next two panels show the approximations to $\dot{\eta}$ and $\ddot{\eta}$, where

$$\begin{aligned} \dot{\eta}^{**}(n) &= [\eta^*(n+1) - \eta^*(n-1)]/(2T) \\ \ddot{\eta}^{**}(n) &= [\dot{\eta}^*(n+1) - \dot{\eta}^*(n-1)]/(2T) \end{aligned} \tag{8-1}$$

The pairs of curves in the bottom panels are again practically indistinguishable; hence we have consistency: $(\dot{\eta}^*, \ddot{\eta}^*)$ are good approximations to the time derivatives of $(\eta^*, \dot{\eta}^*)$. It may be noted that there are leading and trailing transients, such as before $t = 4$ and after $t = 18$. That effect is even more pronounced in figure 12, where improved command x^c (solid line) is compared with the original command x^0 that ignores the zero dynamics. In the figure the pure feedback solution is shown dotted. It is a copy from figures 5 and 6. A noteworthy beneficial effect is that the corrected command is smaller, smoother, and gentler than x^0. The tracking errors are shown in figure 13. They have been reduced by a factor of 20. Thus, we obtain better tracking by means of gentler commands.

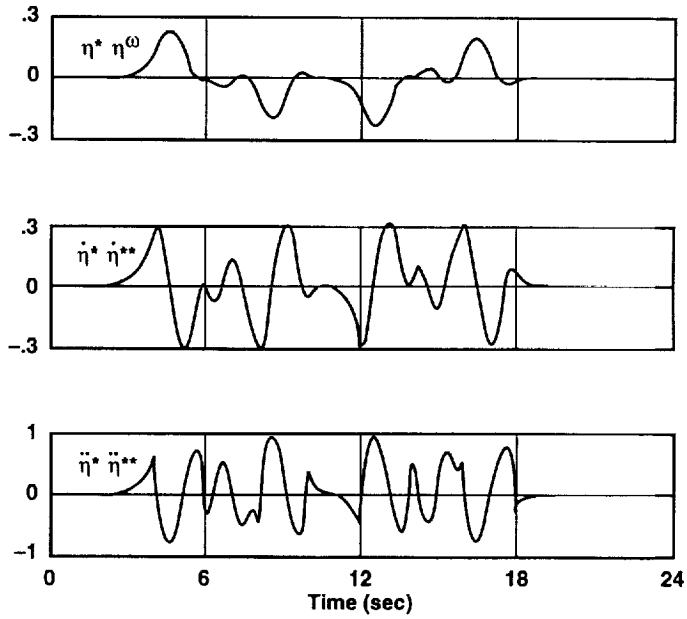

Figure 11. Numeric solution of the zero dynamics.

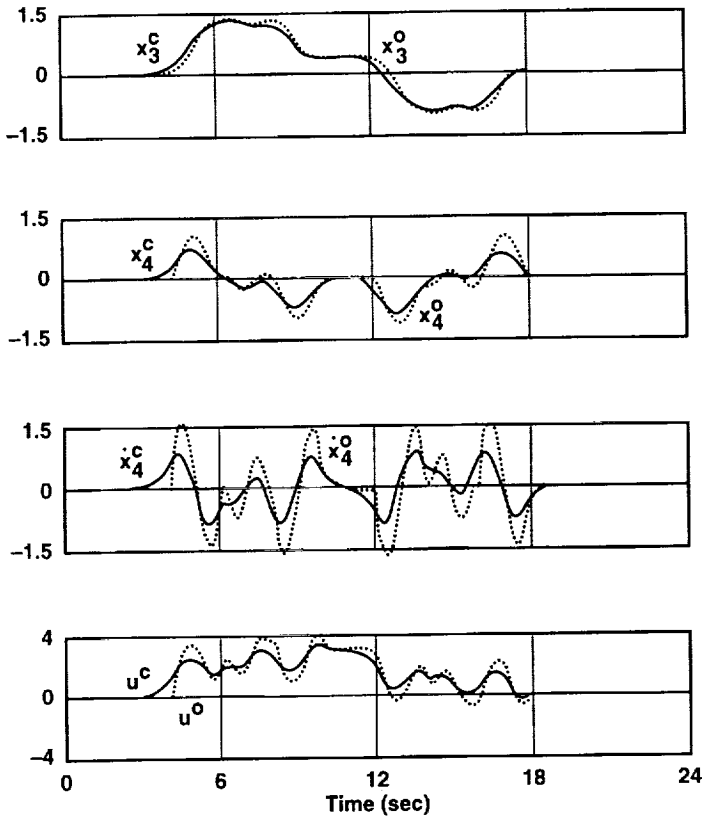

Figure 12. Corrected guidance command.

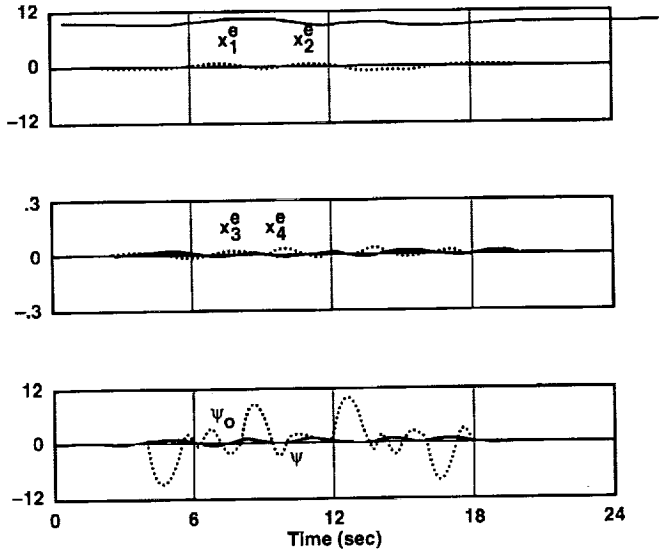

Figure 13. Error response to corrected guidance command.

Linear Time-Varying Example

The state equation in this example is

$$\dot{x} = \begin{pmatrix} 0 & 1 & 0 & 0 \\ 0 & -0.1 & 32.2 & -10.18 \\ 0 & 0 & 0 & 1 \\ 0 & 0 & 0 & 0 \end{pmatrix} x + \begin{pmatrix} 0 \\ p(t) \\ 0 \\ 1 \end{pmatrix} u \tag{8-2}$$

The corresponding zero dynamics are given by (see eq. (4-11))

$$p(t)\ddot{\eta} - 10.18\dot{\eta} + 32.2\eta = -\psi_0 \tag{8-3}$$

The root locus for $-3.22 \leq p \leq 3.22$ is shown in figure 14. At $p = -3.22$ there is a saddle, one root being close to -5 and the other close to $+2$. As p increases, the stable root goes off to $-\infty$ (at $p = 0$ there is a drop in order!) and reappears from $+\infty$ while the unstable root passes through 3. The roots meet for $p = 0.8$, resulting in a repeated unstable pair near $+6$. Then the zero dynamics turn into an unstable spiral. At $p = 3.22$, the roots rest at $(1.58 \pm j2.74)$.

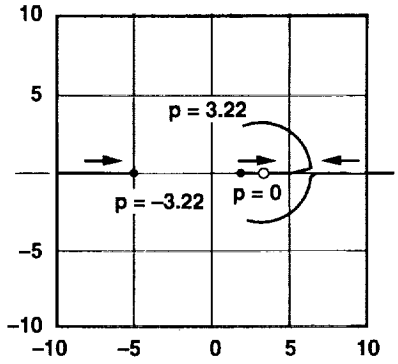

Figure 14. Root locus.

We wish to guide the system along the same trajectory y_c as shown in figure 4, except that the parameter p is changed as shown in figure 15. The system error response without correcting for zero dynamics is shown in figure 16, and the system error response with corrections for zero dynamics is shown in figure 17. It should be noted that an order of magnitude improvement is obtained despite time variation of the zero dynamics. The corrections were implemented in frequency domain. The following noncausal transfer function was used to compute $\eta(t)^{\omega}$.

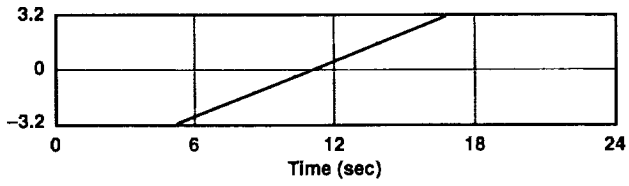

Figure 15. Variation of p.

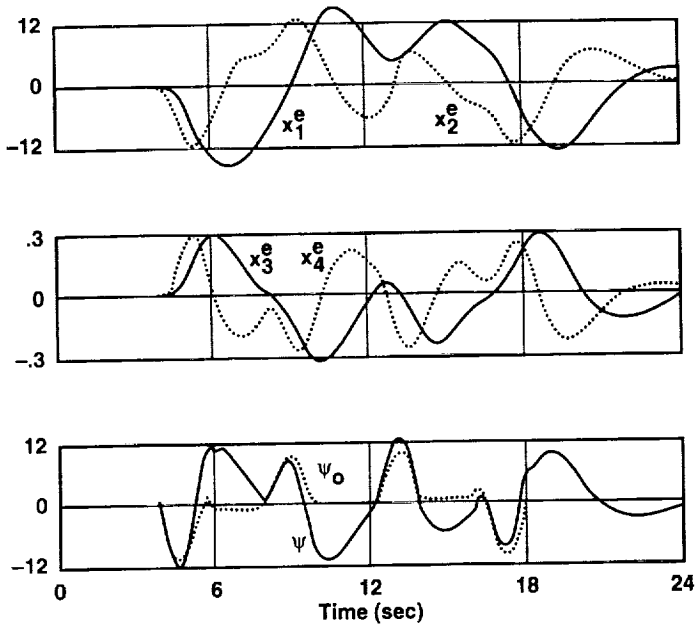

Figure 16. Error response without corrections.

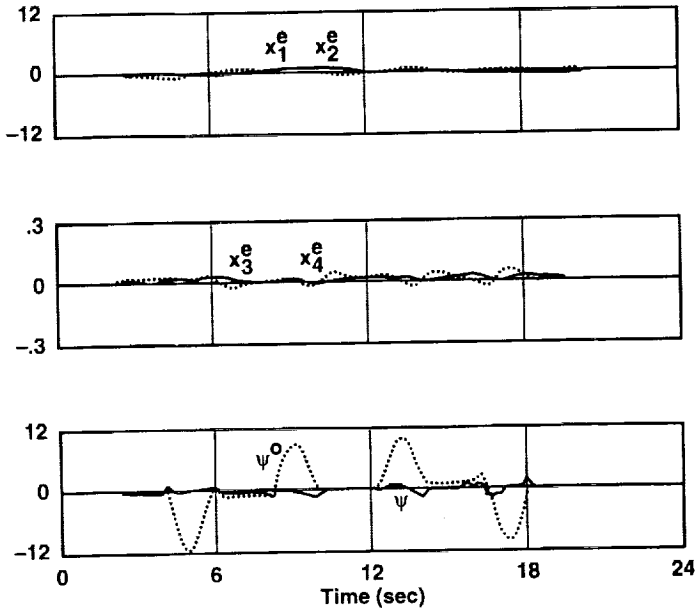

Figure 17. Error response to corrected guidance command.

$$G_0(j\omega) = [p(j\omega)^2 - 10.18(j\omega) + 32.2]^{-1}[1 + (\omega/8)^4]^{-1} \tag{8-4}$$

where p is locally frozen (see below). The derivative $\dot{\eta}(t)^\omega$ was computed by means of $G_1(j\omega) = j\omega G_0(j\omega)$. Rapid frequency roll-off without phase lag was provided by the noncausal filter with the pole pattern shown in figure 18. The filter requires a look-ahead/look-back of 0.5 sec, but since we are already prepared to look-ahead/look-back 2 sec, the noncausal nature of the filter is not a problem. The $g_0(kT), -40 \leq k \leq 40$, needed in the convolution for η^ω, and $g_1(kT), -40 \leq k \leq 40$, needed for $\dot{\eta}^\omega$, were computed every fifth sample using the value of p at the beginning of each quintet.

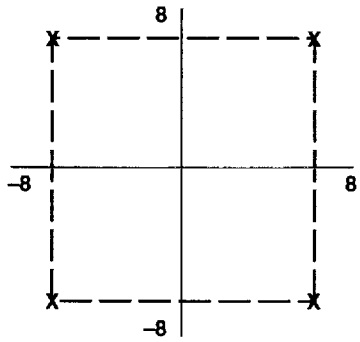

Figure 18. Roll-off filter poles.

Nonlinear Time-Varying Example

The model used next is motivated by the fact that generally the aircraft force and moment generators stiffen with speed. We multiply the linear force and moment used in the preceding example by a factor that is quadratic in speed x_2 to obtain the following nonlinear state equation.

$$\begin{aligned}
\dot{x}_1 &= x_2 \\
\dot{x}_2 &= f_2 = (a_{21}x_1 + a_{22}x_2 + a_{23}x_3 + a_{24}x_4 + a_{25}u + a_{26}p)[1 + (a_{27}x_2)^2] \\
\dot{x}_3 &= x_4 \\
\dot{x}_4 &= f_4 = (a_{41}x_1 + a_{42}x_2 + a_{43}x_3 + a_{44}x_4 + a_{45}u + a_{46}p)[1 + (a_{47}x_2)^2] \\
y &= x_1
\end{aligned} \tag{8-5}$$

The maneuver to be executed is the same as before (fig. 4). With $a_{27} = a_{47} = 0.01$, the multiplying factor ranges from 1 to 2.5. Figure 19 shows the spectrum (λ_1, λ_2) of the zero dynamics with Jacobian matrices frozen at each sample. Both zeros move out with increasing x_2. Also shown are the regulator gains, varied so that the closed-loop poles of the perturbation model with frozen Jacobian matrices at each sample remain, as before, at 0.8 and 2 rad/sec, both with 0.5 damping. The tracking errors after only one iteration ($\gamma = 1$) are shown in figure 20; they are small. It is particularly noteworthy that the acceleration error of the corrected guidance ψ (solid line) is an order of magnitude smaller than the pure feedback error ψ_0 (dotted line).

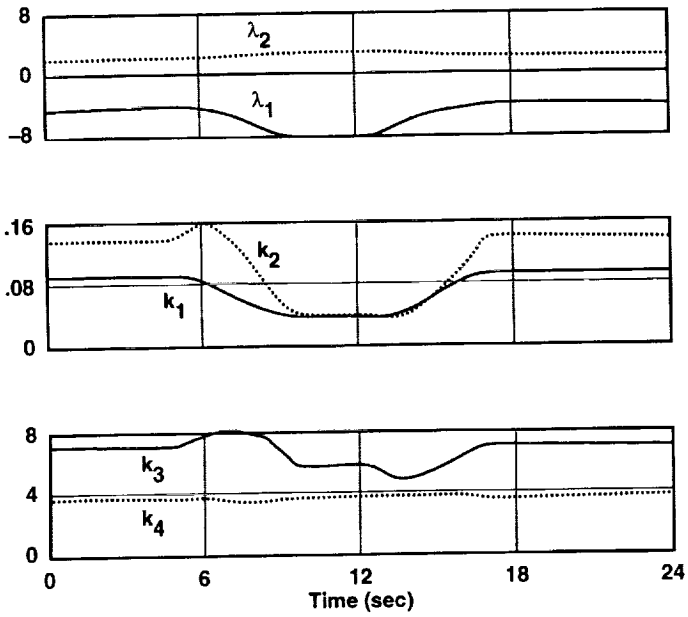

Figure 19. Variation of zeros and regulator gains.

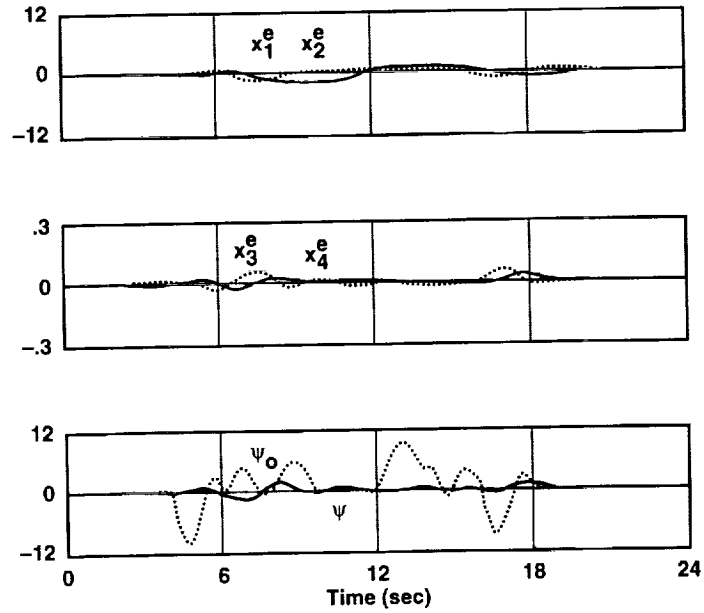

Figure 20. Error response of nonlinear system.

9 Conclusion

An algorithm for computing state trajectories and controls that guide a nonlinear system through given sequences of control points has been presented. It is assumed that the control point schedule is known several points in advance. In the algorithm, the control points are linked by polynomial segments. The first approximation of the guiding state trajectory is obtained by equating the system output with the polynomial schedule and inverting the pure feedback part of the system. In the presence of zero dynamics this first approximation will produce acceleration errors. A correction is obtained by means of the stable, steady state solution of the local zero dynamics. If nonminimum phase zeros are present, future values of the approximate solution are used. Numerical tests indicate that an order-of-magnitude reduction in the acceleration error is possible with look-ahead of only four times the time constant of the unstable zero. Therefore, the control points must be available that much in advance. Usually, this does not pose a problem in the fully automatic mode of operation of the system, since the higher-level planner that provides the control point schedule has a much wider horizon than the servosystem being discussed here. Although a regulation process must always be causal, a guidance process may employ noncausal computations.

10 References

1. Meyer, G.; and Cicolani, C.: Application of Nonlinear Systems Inverses to Automatic Flight Control Design. Theory and Applications of Optimal Control in Aerospace Systems, P. Kant, ed., AGARDograph No. 251, 1981.

2. Smith, G. A.; and Meyer, G.: Aircraft Automatic Flight Control System with Model Inversion, Control and Dynamic Systems, C. T. Leondes, ed., vol. 38, 1990, pp. 1–40.

3. Isidori, A.; and Byrnes, C.: Output Regulation of Nonlinear Systems. IEEE Trans. on Automatic Control, vol. 35, no. 2, 1990, pp. 131–140.

4. Paden, B.; and Chen, D.: A State-Space Condition for the Invertibility of Nonlinear Nonminimum-Phase Systems. Advances in Robust and Nonlinear Control Systems, DSC-vol. 43, ASME, 1992. pp. 37–41.

5. Paden, B.; Chen, D.; Ledesma, R.; and Bayo, E.: Exponentially Stable Tracking Control for Multijoint Flexible-Link Manipulators. J. Dynamic Systems, Measurement, and Control, ASME Trans., vol. 115, Mar. 1993, pp. 53–59.

6. Devasia, S.; and Paden, B.: Exact Output Tracking for Nonlinear Time-Varying Systems. Paper TP11.2, Proc. 33rd Conf. on Decision and Control, Lake Buena Vista, Fla., Dec. 14–16, 1994.

7. Meyer, G.; and Smith, G. A.: Dynamic Forms Part I: Functions. NASA TP-3397, Aug. 1993.

8. Isidori, A.: Nonlinear Control Systems: An Introduction. Springer-Verlag, New York, 1989.

9. Ästrom, K. J.; and Wittenmark, B.: Computer Controlled Systems Theory and Design, Prentice-Hall, Englewood Cliffs, N.J., 1984.

10. FORTRAN Subroutines for Mathematical Applications, Version 2.0, IMSL, Inc., 1991.

REPORT DOCUMENTATION PAGE

Form Approved
OMB No. 0704-0188

1. AGENCY USE ONLY *(Leave blank)*	2. REPORT DATE	3. REPORT TYPE AND DATES COVERED
	January 1995	Technical Memorandum

4. TITLE AND SUBTITLE

Nonlinear System Guidance in the Presence of Transmission Zero Dynamics

5. FUNDING NUMBERS

505-64-52

6. AUTHOR(S)

G. Meyer, L. R. Hunt, and R. Su

7. PERFORMING ORGANIZATION NAME(S) AND ADDRESS(ES)

Ames Research Center
Moffett Field, CA 94035-1000

8. PERFORMING ORGANIZATION REPORT NUMBER

A-95014

9. SPONSORING/MONITORING AGENCY NAME(S) AND ADDRESS(ES)

National Aeronautics and Space Administration
Washington, DC 20546-0001

10. SPONSORING/MONITORING AGENCY REPORT NUMBER

NASA TM-4661

11. SUPPLEMENTARY NOTES

Point of Contact: G. Meyer, Ames Research Center, MS 210-3, Moffett Field, CA 94035-1000; (415) 604-5750

12a. DISTRIBUTION/AVAILABILITY STATEMENT

Unclassified — Unlimited
Subject Category 31

12b. DISTRIBUTION CODE

13. ABSTRACT *(Maximum 200 words)*

An iterative procedure is proposed for computing the commanded state trajectories and controls that guide a possibly multiaxis, time-varying, nonlinear system with transmission zero dynamics through a given arbitrary sequence of control points. The procedure is initialized by the system inverse with the transmission zero effects nulled out. Then the "steady state" solution of the perturbation model with the transmission zero dynamics intact is computed and used to correct the initial zero-free solution. Both time domain and frequency domain methods are presented for computing the steady state solutions of the possibly nonminimum phase transmission zero dynamics. The procedure is illustrated by means of linear and nonlinear examples.

14. SUBJECT TERMS	15. NUMBER OF PAGES
Automatic control, Nonlinear, Dynamic systems	48
	16. PRICE CODE: A03

17. SECURITY CLASSIFICATION OF REPORT	18. SECURITY CLASSIFICATION OF THIS PAGE	19. SECURITY CLASSIFICATION OF ABSTRACT	20. LIMITATION OF ABSTRACT
Unclassified	Unclassified